

# Multi-Temporal Sentinel-2 Images for Classification Accuracy

Yuhendra and Eva Yulianti

Department of Informatics Engineering, Padang Institute of Technology, Padang (West Sumatera), Indonesia

## Article history

Received: 06-12-2018

Revised: 07-02-2019

Accepted: 21-02-2019

Corresponding Author:

Yuhendra

Department of Informatics  
Engineering, Padang Institute  
of Technology, Padang (West  
Sumatra), Indonesia

Email: yuhendra@ieee.org

**Abstract:** The term ‘multi-temporal’ refers to data recorded by sensors scanning the same scene at different dates and times. In this research, Sentinel-2A images were selected for the analyses. Sentinel-2 is a very new program of the European Space Agency (ESA) designed for fine spatial resolution global monitoring. Land Cover–Land Use (LCLU) classification tasks can take advantage of the fusion of radar and optical remote sensing data, generally leading to increased mapping accuracy. Here we propose a methodological approach to fuse information from the new European Space Agency Sentinel-1 and Sentinel-2 imagery for accurate land cover mapping of a portion of the South Solok region, West Sumatra. Data pre-processing used the European Space Agency’s Sentinel Application Platform and the SEN2COR toolboxes. The two main objectives of this study are to evaluate the potential use and synergetic effects of ESA Sentinel-1A C-band SAR and Sentinel-2A Optical data for classification and mapping of LCLU. First, the pre-processing chain supported by sensor-specific toolboxes developed by ESA represents a reliable and fast approach for the preparation of ready-to-process imagery. Second, an investigation to derive a methodological framework to integrate Sentinel-1 and Sentinel-2 imagery for land cover mapping by integrating radar and optical imagery has been set up and tested. The results of object-based classification produced higher accuracy than pixel-based classifications if the same type of classifier is used. The classifier algorithms using k-Nearest Neighbors (k-NN) function performed slightly better, with an overall accuracy of 91.30%.

**Keywords:** Sentinel Image, SAR, LULC, Data Fusion, South Solok

## Introduction

South Solok is in the Bukit Barisan mountains and in the Watermelon fault area of Indonesia. The region is located at 01°17'13"-01°46'45" South Latitude and 100°53'24"-101°26'27" East Longitude. It covers an area of around 3,590 Km<sup>2</sup> and occupies the southern part of West Sumatra. Administratively, the Government of South Solok consists of seven sub-districts and 32 Nagari. The district has a lot of natural resources that provide development through mining, plantations and agriculture. Gaining an accurate picture of Land Use and Land Cover (LULC) is an important part of the planning or implementation of development projects. The demand for LULC mapping has led the government to monitor natural resources potential regularly. For example, agricultural areas change significantly during a growing season because of phenology. Remote Sensing (RS), specifically Synthetic Aperture Radar (SAR) image radar, is more effective at land cover mapping in

comparison with ground surveying methods. This is because radar is more sensitive to physical structures like crops and the water content of biomass/vegetation.

Innovations in remote sensing allow testing to be carried out using active Synthetic Aperture Radar (SAR) or passive (optical and thermal range, multispectral and hyperspectral). SAR can penetrate clouds and can perform land cover mapping with or without sunlight. Remote sensors are regularly used in landslides, subsidence, or to identify types of vegetation and to observe changes to land cover. Satellite data and high-resolution imagery (Landsat, Sentinel, Spot, QuickBird) help to overcome certain limitations of RS by improving processes like image sharpening, classification of land, detection of changes and object identification. Recently, high-resolution RS data are considered indispensable for monitoring essential aspects of the Earth’s surfaces (Li *et al.*, 2011; Yuhendra, 2017; Yuhendra *et al.*, 2012). For the high-resolution image, an optical image from Sentinel-2 is used along with the SAR image from Sentinel 1A.

**Table 1:** Detail of information spectral bands of sentinel-2 images

Sentinel- 2A (Optical Data)					
Band No	Wavelength (µm)	Spatial Resolution (m)	Band No	Wavelength (µm)	Spatial Resolution (m)
1	0.43-0.453	60	7	0.765-0.785	20
2	0.458-0.523	10	8	0.785-0.900	10
3	0.543-0.578	10	8a	0.855-0.875	20
4	0.650-0.680	10	9	0.930-0.950	60
5	0.698-0.713	20	10	1.365-1.385	60
6	0.7330.748	20	11	1.565-1.655	20

Sentinel-2 was introduced by the ESA to perform global spatial resolution monitoring as part of the EUs Copernicus program (Manaf *et al.*, 2016; Hagolle *et al.*, 2015; Segl *et al.*, 2015). Sentinel-2 images cover 13 wavelengths in the visible, Near Infrared (NIR) and Shortwave Infrared (SWIR). The bands are at 10, 20 and 60 m spatial resolutions (Table 1) and the sensor has a field of view of 290 km. This field of view is much larger than the established Landsat sensor, which only has a view of 185 km<sup>4</sup>. The data produced by the Sentinel-2 data is used to support various activities like crop monitoring and land classification. Due to the limitations of optical SAR image processing, scientists are increasing efforts to refine and improve remote sensing (Segl *et al.*, 2015; Wang *et al.*, 2016; Fernández-Manso *et al.*, 2016; Immitzer *et al.*, 2016; Novelli *et al.*, 2016; Storey *et al.*, 2016; Van der Werff and Van der Meer, 2016). In image fusion applications, the fusion of sensor data can help RS perform better at classifying land, detecting changes, identifying objects, segmenting images, updating maps and monitoring hazards (Li *et al.*, 2011; Yuhendra, 2017; Yuhendra *et al.*, 2012). This research examines multi-temporal Sentinel-1 (SAR) and Sentinel-2 (Optical) satellite data, for land cover mapping and classification. Some publications focus on the multi-temporal image fusion and application (Gao *et al.*, 2017; Ghassemian, 2016; Zhuang *et al.*, 2018; Patrick *et al.*, 2018; Kandrika and Ravinsankar, 2011). Multi-temporal data fusion is essential for detecting changes and helps to provide more accurate classifications. Land cover mapping of built-up environments is not straightforward because it is sometimes hard to differentiate between natural and non-natural features. Urban land cover mapping is usually carried out using medium-resolution multispectral data (Wurm *et al.*, 2011). This study uses a combination of data from Sentinel-1 and Sentinel-2 to map South Solok accurately. By combining the benefits of radar and optical imaging and through the use of object-based and spectral classification, this study proposes an inexpensive and accurate method to map land cover.

## Research Methods

### Study of Specific Area

The region that was studied for this research is situated in South Solok, in West Sumatra, Indonesia

(Fig. 1). The total area is 3.346,20 km<sup>2</sup>. It is near Bukit Kunyeng, Siruek and Bukit Gadang. Solok Selatan has a population of approximately 144,000. It is situated at 1°14' (1.2333°) south and longitude 101°25'1.2" (101.417°) east.

### Satellite Dataset

Sentinel-1 consists of two satellites that were developed by the ESA and financed by the European Commission. It orbits the poles and provides round the clock SAR imaging from an altitude of 700 km. Sentinel-2 was launched in April of 2014 and 2016 and is used for land-cover and land-use mapping and change detection). Both Sentinel- 2a and 2b use an MSI (Multispectral Imagery) instrument (He *et al.*, 2017) to produce imagery with 13 spectral bands.

For this study, Sentinel-2 data is taken using a temporal resolution of ten days for the first satellite and five days with the two other satellites. These time frames provide sufficient observation data with varying spatial resolutions of between 10 m to 60 m. The data used in this study is comprised of three elements. They are one SAR image taken from Sentinel-1 and two optical images produced by Sentinel-2. The images cover the principal areas of South Solok and are provided in Table 2.

### SAR Satellite Data (Sentinel-1A)

Sentinel-1A launched in April of 2014 and Sentinel-1B two years later in 2016. Sentinel-1A data (level 1 product) carries a C-band SAR instrument and has four operational modes: Interferometrics wide-swath (IW), with a swath width of 250 km and 5×20 m<sup>2</sup> pixel resolution; wave-mode (WV), at 20×20 km<sup>2</sup> and 5×5 m<sup>2</sup> pixel resolution; strip map (SM) mode, at 80 km swath width and 5×5 m<sup>2</sup> pixel resolution; and Extra Wide-swath (EW), at 400 km swath width and 20×40 m<sup>2</sup> pixel resolution. The satellite supports operations in a single (HH or VV) or dual polarisation (VV + VH or HH + HV). Each Sentinel-1 product acquired in SM, IW and EW can be distributed at three processing levels: (i) Level-0 products are compressed, unfocused SAR data in its raw form and is vital in the production of higher-level products. (ii) Level-1 products are focused on data and are designated for most data users. Processing from level-0 to level-1 includes Doppler centroid estimation,

single look complex focusing and image and post-processing for the Single Look Complex (SLC) and Ground Range Detected (GRD) products. The SLC and GRD are two different level-1 sub-products. (iii) Level-2 consists of geo-located geophysical products derived from Level-1 (Navarro *et al.*, 2016; Zhou *et al.*, 2018). For this research, one Sentinel 1A image (Level 1 product) that covered the desired area was acquired from the ESA’s Sentinel Scientific Hub, (Fig. 3a).

*Optical Satellite Data (Sentinel 2-A)*

The Sentinel-2 mission consists of two satellites and produces imaging using 13 spectral bands at an altitude of 786 km. Sentinel-2A was launched June 23, 2015. All data acquired by the satellite sensor is processed at various levels. Sentinel-2A images were selected for this study because they are the best of what is available from the ESA. The first one, level-0, includes telemetry analysis, of low-resolution image extraction and ancillary telemetry analysis, among others. The second one, level-1, is produced by using level-0 output and has three different sub-products: (i) Level-1A, which decompresses relevant mission source packets; (ii) level-1B, which applies radiometric corrections to level-1A output; and (iii) level-1C, where radiometric and geometric corrections (including ortho-rectification and spatial registration) are performed and Top of the Atmosphere (TOA) are calculated. The third one, Level-

2, includes a scene classification and an atmospheric correction applied to TOA values among others. Sentinel 2-A can be processed on the user side through specific software (Sentinel-2 Toolbox). In this research, two scene data Sentinel-2A (optical) were acquired on June 13, 2017 (scene 1) and October 18, 2017 (scene 2), downloaded from the ESA’s Sentinel Scientific Hub products (<https://schub.copernicus.eu/>) (Fig. 3b and 3c). Sentinel-2A consists of 13 spectral bands with four bands at 10 m: the classical blue (490 nm), green (560 nm), red (665 nm) and NIR (842 nm) bands dedicated to land applications; six bands at 20 m: Four narrow bands in the vegetation red edge spectral domain (705 nm, 740 nm, 775 nm and 865 nm); two SWIR large bands (1610 nm and 2190 nm) dedicated to snow/ice/cloud detection; to vegetation moisture stress assessment; three bands at 60 m dedicated to atmospheric correction (443 nm for aerosols and 940 for water vapour); and to cirrus detection (1380 nm). Details of Information Spectral Bands of Sentinel-2 Images are given in Table 1 and Fig. 2.

**Table 2:** Detail of Acquisition Information on experimental Sentinel-2 data sets

Satellite data	Acquisition time
SAR image (Sentinel 1A)	28 February 2018
Optical image (Sentinel 2A)	13 June 2017
	18 October 2017

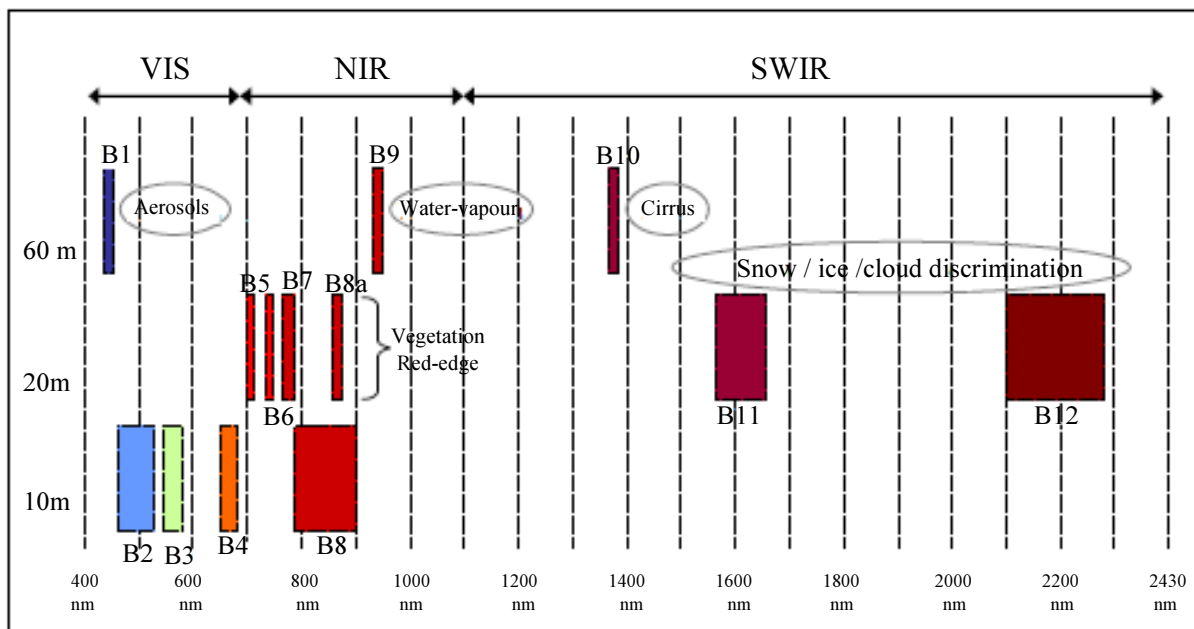


**Fig. 1:** Multi Spectral band of Sentinel-2A

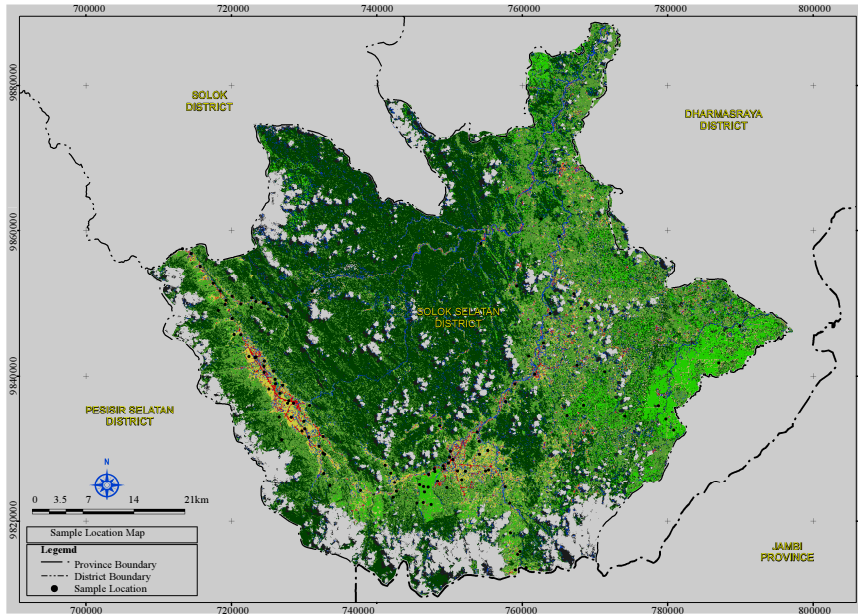


**Fig. 2:** Map of location research area in South Solok, West Sumatra

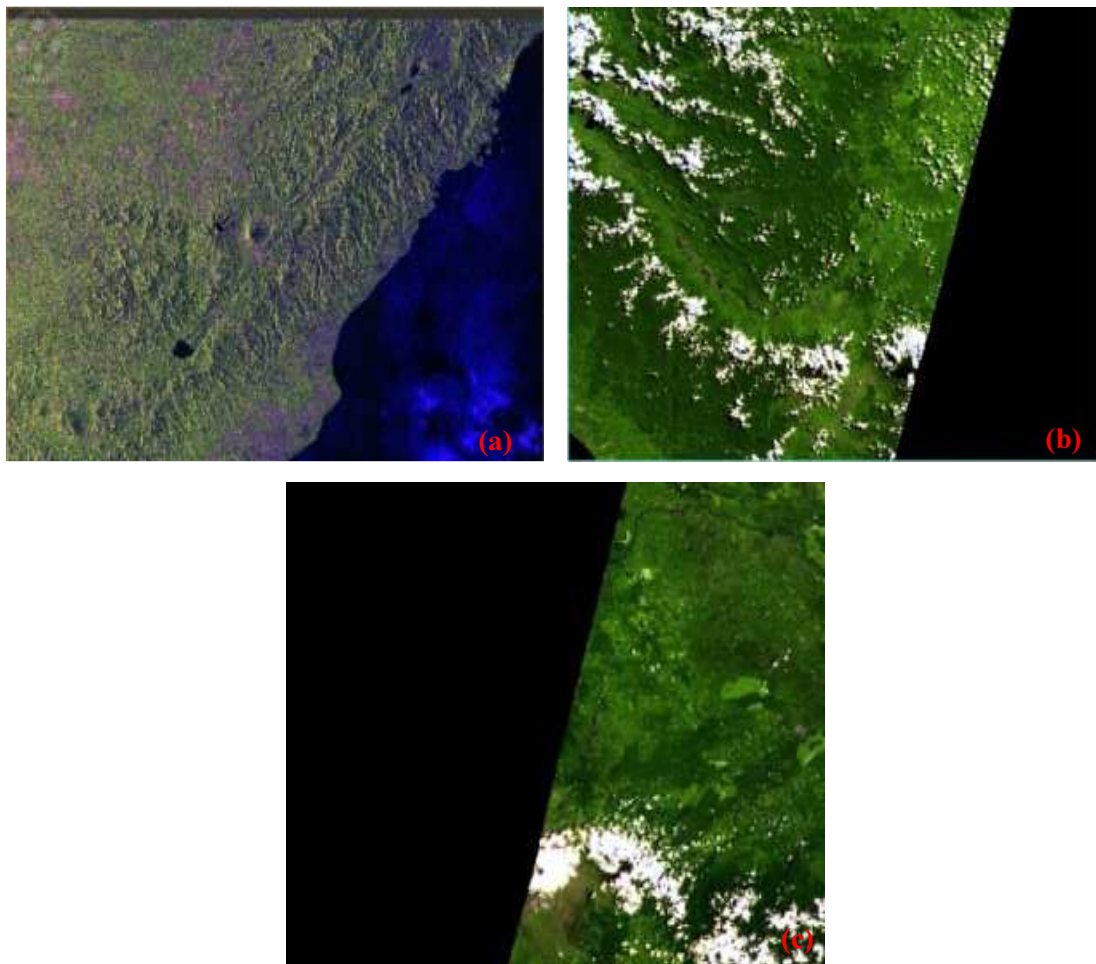


**Fig. 3:** (a) Sentinel-1A image (b-c) Sentinel-2A images

### Satellite Data Pre-Processing

This research was conducted in several steps designed to show a framework of Sentinel-2 images fusion. Stages in this research are shown in Fig. 4.

#### Pre-Processing Sentinel-1A

- Radiometric and Topographic correction: Radiometric correction and terrain correction/topography using Sen2Cor toolbox with the Sentinel Application Platform (SNAP)
- Image calibration, Thermal Noise Removal and TOPSAR Deburst: The system must be calibrated since the image contains many invalid pixel values. It needs to get real object pixel value on the surface of the Earth and will produce Sentinel-1A Level-1 satellite image with Sigma0\_VH and Sigma0\_VV polarisation
- Terrain Correction: Using Doppler Range, this method uses vector information of satellite orbit state, imaging time, satellite angle conversion parameters to the surface of the earth and Digital Elevation Model (DEM) data to obtain an exact location on the surface of the Earth. DEM using with 30 m spatial resolution with the re-projection image was performed using UTM Zone 47S and using WGS 1984
- Re-sampling: In which each data point (pixel) in the high-resolution base map is assigned a value depending on the MS image pixels. For optimum results, Sentinel-2 images need to be re-sampled with spatial resolution  $10 \times 10 \text{ m}^2$ . Bilinear Interpolation re-sampling is a popular method, but it can affect the precision of the image
- Speckle (Image filtering): A scattering phenomenon and not noise. The discrimination of different natural

media by comparing intensity to a fixed threshold leads, in general, to numerous errors due to the high variability of SAR speckled response. The analysis of the image used Lee filter with kernel  $5 \times 5$

#### Pre-Processing Sentinel-2A

Below the stages of Sentinel-2A satellite images processing are described:

- Atmospheric Correction: Used to remove the influence of atmospheres (molecules and particles) participating in scattering the signal before a remote sensing sensor records. The software processing uses SEN2COR toolbox. A result of image correction is shown in Fig. 5
- Re-sampling: Sentinel-1A images should be re-sampled with spatial resolution  $10 \times 10 \text{ m}^2$  with bilinear interpolation
- Layer stacking and Cropping: Layer stacking is the process of making a multi-band image by combining images from separate bands into one file. Sentinel-1A Level-1 has been calibrated with Sigma0\_VH and Sigma0\_VV polarisation

#### Object-Based Classification and Segmentation

In this research, object-based classification (segmentation) was performed using Trimble's eCognition® v.9.01 software with a user-supervised parameterisation. This software segments the images into homogeneous objects and uses information derived from each object in the classification (Zhou and Zheng, 2017). The eCognition software is the first commercially available product for object-oriented and multi-scale image analysis.

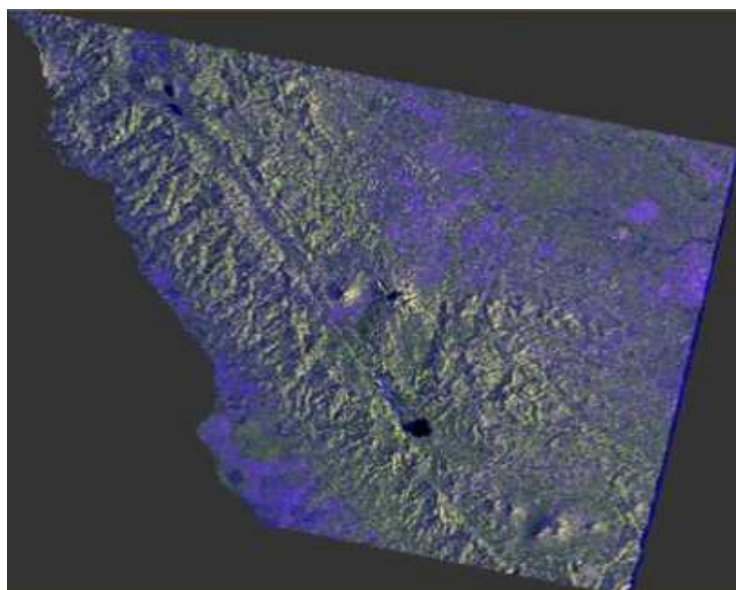


Fig. 4: Result of the image with radiometric and terrain corrected

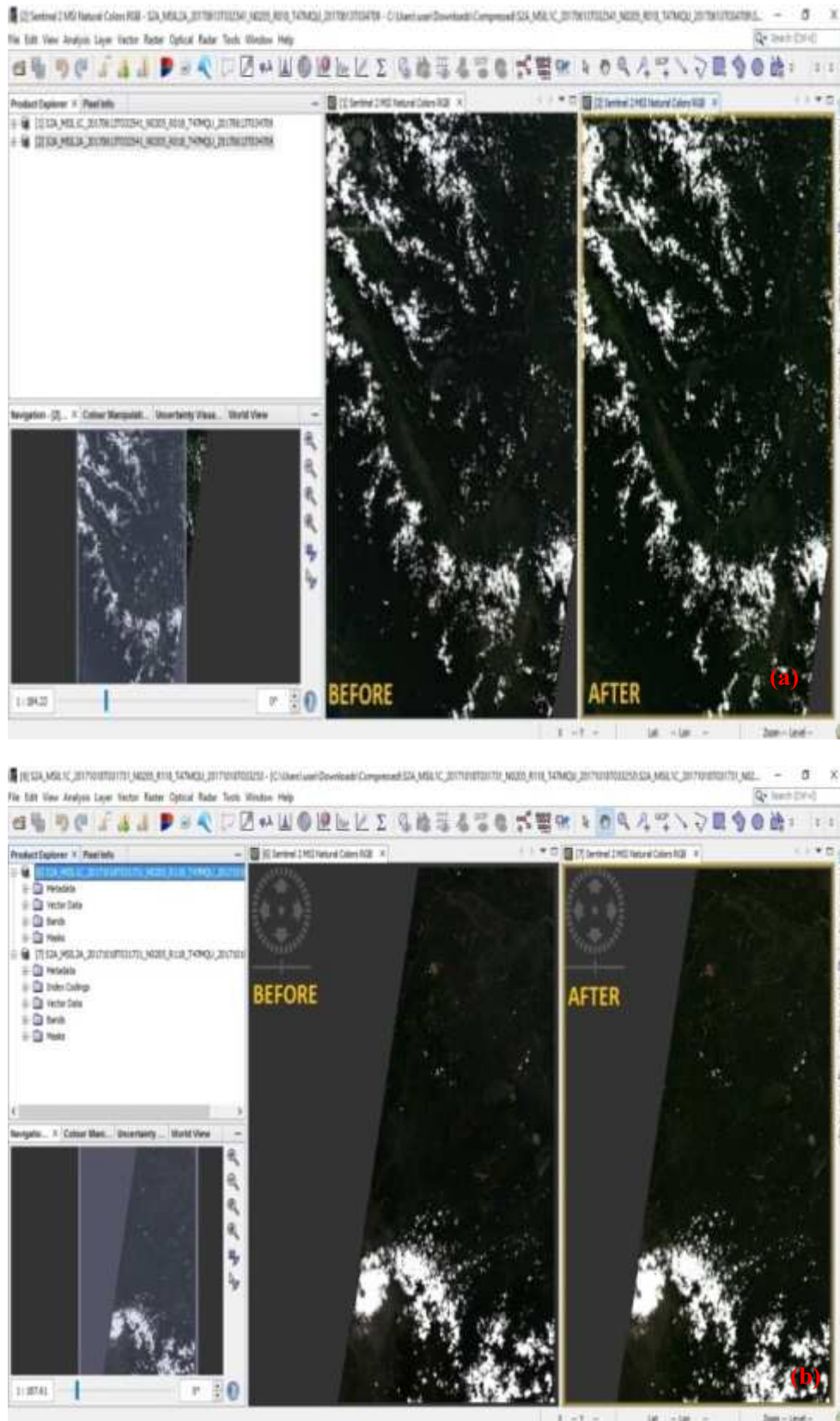


Fig. 5: Atmospheric correction of (a) scene 1, (b) Scene 2 of sentinel-2A image

It is designed to work on high spatial resolution or hyper-spectral imagery and includes several useful parameters to develop a knowledge base for elaborate land use classification. The principal procedure of recognition is focused on multi-resolution segmentation and a patented image object extraction. Each level in this hierarchical network is produced by a single segmentation processing. The whole image analysis process can be divided into the two principal workflow steps: Segmentation and classification (Chhetri *et al.*, 2017). Segmentation means the process of grouping like elements by homogeneity and merging them into distinct regions. To obtain segments suited for the desired classification, the segmentation process can be manipulated by defining which of the loaded channels are to be used by what weight and by the following three parameters: Scale, colour and form. Smoothness describes the similarity between the image object borders and a perfect square while compactness describes the closeness of pixels clustered in an object. Sample selection is the final key process for performing a successful classification in eCognition. Choosing representative samples is critically important as they define the range of spectral signatures and image object properties that group other objects into the classification categories. Classification algorithms were tested using k-Nearest Neighbours (k-NN) function. The function is applied to the samples and image objects are sorted into the appropriate category based upon best fit to the selected samples.

#### Accuracy Assessment

In this research, nine different urban land cover types were identified: Forest, Vegetation, Plantation, Agriculture Mixed, Agriculture, Urban, Bare Soil, Rice Field, Water Body. In RS application, accuracy assessment is an important part in the classification process. Classification accuracy assessment is commonly expressed using a metric computed from the error or confusion matrix using the testing set (Li *et al.*, 2011). The phase of classification accuracy testing was done by an accuracy testing method using the Kappa coefficient. This accuracy uses all elements in the confusion matrix. The Kappa coefficient is based on the consistency of the assessment by considering all aspects. There are several accuracy assessment percentages that can be calculated, including accuracy (omission error), user accuracy (commission error) and overall accuracy obtained from the error matrix or confusion matrix (Yuhendra, 2017; Baumann *et al.*, 2012; Bargiel, 2017). Through matrix error (confusion matrix), user accuracy, the producer's accuracy, overall accuracy, the Kappa coefficient (Kappa coefficient) can be obtained mathematically in the following ways.

*User Accuracy* is a measurement indicating the probability that a pixel is a class A, given that the classifier has labelled the pixel into Class A:

$$User\ accuracy = \frac{Number\ of\ correct\ classifications}{Total\ number\ of\ classification} \times 100\% \quad (1)$$

*Error Commission:*

$$Error\ Commission(\%) = 100 - User\ Accuracy \quad (2)$$

*Procedure Accuracy* is a measure of how much of the land in each category was classified correctly:

$$Procedure\ accuracy = \frac{Number\ of\ correct\ classification}{Total\ number\ of\ classification} \times 100\% \quad (3)$$

*Error Omission:*

$$Error\ omission(\%) = 100\% - Producer\ accuracy \quad (4)$$

Overall Accuracy (OA) is calculated by summing the number of pixels classified correctly and dividing by the total number of pixels. The ground truth image or ground truth ROIs define the true class of the pixels.

The pixels classified correctly are found along the diagonal of the confusion matrix table, which lists the number of pixels classified into the correct ground truth class. The total number of pixels is the sum of all the pixels in all the ground truth classes:

$$Overall\ accuracy = \frac{Number\ of\ pixel\ classified\ correctly}{Total\ number\ of\ pixel} \times 100\% \quad (5)$$

Coefisien Kappa ( $\kappa$ ) is another measurement of the classification accuracy. It is calculated by multiplying the total number of pixels in all the ground truth classes (N) by the sum of the confusion matrix diagonals ( $\sum^x \sum^k x_{kk}$ ), subtracting the sum of the ground truth pixels in a class times the sum of the classified pixels in that class summed over all classes ( ) and dividing by the total number of pixels squared minus the sum of the ground truth pixels in that class times the sum of the classified pixels in that class summed over all classes:

$$\kappa = \frac{N \sum_k x_{kk} - \sum_k x_k \sum^x \sum^k}{N^2 - \sum_k x_k \sum^x \sum^k} \quad (6)$$

The research proposed has tested and validated 115 land cover land use class sample spreads on the location. The sample of accuracy test is shown in Table 3.

**Table 3:** Distribution of training and validation data for each class

Class	NTP*	NPV**	NTT***	NE****	NV*****
Forest	13	13	115	10	105
Vegetation	10	9			
Plantation	12	11			
Agriculture	10	9			
Mixed Agriculture	12	10			
Urban	16	15			
Bare Soil	12	11			
Rice Field	19	17			
Water Body	11	10			

\*NTP: Number of Training Pixel, \*\*NPV: Number of Pixel Validation

\*\*\*NTT: Number of Total Training, \*\*\*\*NE: Number of Error

\*\*\*\*\*NV: Number of Valid

## Result and Analysis

### Segmentation

A set of land cover classes of interest were defined, namely: Forests, secondary vegetation/shrubs, cropland/plantation, agriculture, mix agriculture, urban, bare soil, rice fields and water bodies. The land use-land cover categories were selected using common categories described in many studies and functional to the project mapping task; that is, the identification of LCLU. Due to the high heterogeneity present within some land cover classes, especially cropland, this study opted for a classification approach exploiting textural land properties. An object-based classification (segmentation) was performed using eCognition® v.9.01 by a user-supervised parameterisation. Three steps represent the main operations performed: (i) Image

segmentation, (ii) generation of an image object hierarchy and (iii) classification. In this approach, ‘objects’ are defined as exploiting topologic (neighbourhood, context) and geometric (form, size) information. The identification of homogeneous land patches was conducted through a supervised iterative process by tuning the parameters of scale, shape and compactness. A scale in an abstract value to determine the maximum possible change of heterogeneity was caused by fusing several objects. This means that shapes denote compactness (pixels clustered on objects closely) and smoothness (similarity of two images). In the multi-resolution segmentation test, this study developed an optimum segmentation value that was identified with scale = 10, shape = 0.8 and compactness 0.2, and the result was shown in Fig. 6. This study then trained the object-based classifier by assigning a land cover class (labelling).

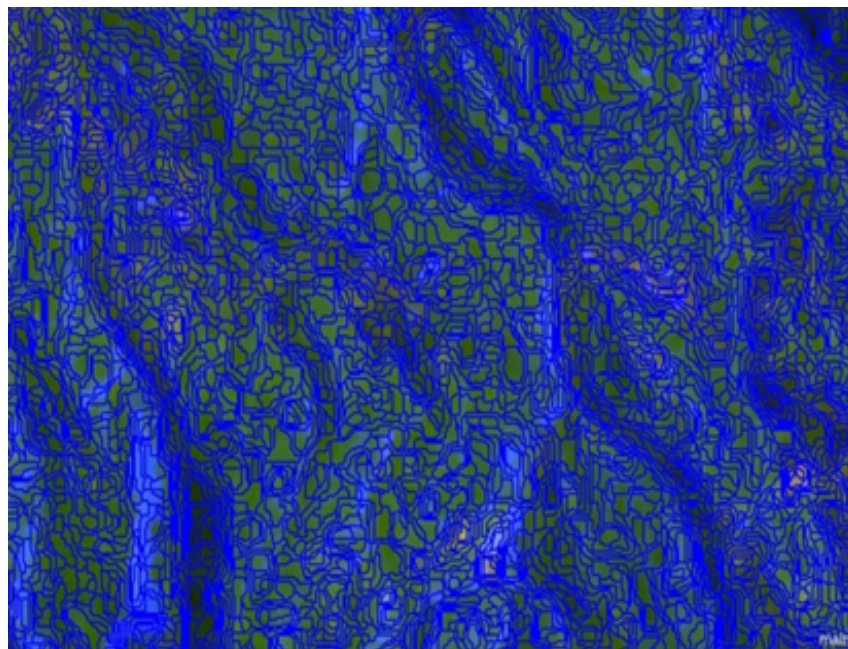


**Fig. 6:** Segmentation image

**Table 4:** Confusion matrix for classification accuracy from Sentinel-2 images

Sample class	PA (%)	UA (%)	EC (%)	EO (%)	OA (%)	KC
Water Body	100.00	90,91	9.09	9,09	91.30	0.89
Forest	100.00	100	0.00	0		
Mixed Agriculture	100.00	83.33	16.67	16,67		
Urban	93.75	100	0.00	0		
Bare Soil	91.66	91.66	8.34	8,34		
Agriculture	91.66	91.66	8.34	8,34		
Plantation	89.47	77.27	22.73	22,73		
Vegetation	90.00	81.81	18.19	18,19		
Rice Field	90.00	90	10.00	10		

PA: Producer's Accuracy; UA: User's Accuracy  
 EC: Error Commission; EO: Error Omission  
 OA: Overall Accuracy; KC: Kappa Coefficient

**Table 5:** Wide of LULC areas in South Solok

No	Class	Wide Area (Ha)
1	Forest	144.775.21
2	Vegetation	837.421
3	Plantation	245.530
4	Agriculture	143.306
5	Mixed Agriculture	191.115
6	Urban	377.045
7	Bare Soil	472.871
8	Rice field	138.683
9	Water Body	183.139
10	Cloud	432.626
11	Shadow Cloud	186.563
	<b>Total</b>	<b>35901487</b>

Classification algorithms were tested using k-Nearest Neighbours (k-NN) assigning the same weight to each layer of the 20 bands layer stack image.

#### Accuracy Assessment and Classification

Table 5 shows the final classification training result based on overall accuracy, kappa coefficients, producer's and user's accuracies for LULC. Table 4 shows the overall accuracy of 91.30% and a high kappa coefficient of 0.89. The wide range of LULC areas in South Solok is 35901487 hectares. The dominant land cover in the study area is followed by forest (144.775.21 hectares), secondary vegetation/shrubs (837.421 hectares) and plantation (245.530 hectares), respectively. A detail wide view of LULC area is shown in Table 5.

#### Conclusion

The results of this study highlight two significant benefits of this type of testing. First, the ESA pre-processing with sensor-specific toolboxes is a quick and reliable method of preparing ready-to-process images. Second, by integrating Sentinel-1A (SAR) and Sentinel-2 (optical) imagery, the benefits of both radar and optical imaging can be exploited. The object-based classification produced accurate and satisfactory results for the LCLU mapping. Sentinel-2 bands are of excellent quality for the applications area

in LULC observation, with more satisfying results. However, one of the limitations depends on user skill experiences in pre-processing and processing the image. For improving the classification accuracy of built-up areas, the study recommends the use of very high-resolution images.

Based on the classification from two satellite images (Sentinel-1A and Sentinel-2A) for LULC identification by object-based classification with the set of segmentation parameter and tested, the values were given for Scale 10, shape 0.8 and compactness 0.2 used the k-Nearest Neighbourhood algorithm of clustering.

#### Acknowledgement

The special thanks to the European Space Agency (ESA) Sentinel Scientific Hub products, for providing the free download Sentinel imagery data; and, especially, for an anonymous reviewer for valuable comments and suggestions.

#### Funding Information

The authors gratefully acknowledge the Ministry of Research, Technology and Higher Education of the Republic of Indonesia for funding this research, with contract No.519/27.O10.4.2/PN/II/2018; the European Space Agency (ESA) Sentinel Scientific Hub products, for providing the free download Sentinel imagery data; and, especially, for an anonymous reviewer for valuable comments and suggestions.

#### Author's Contributions

All author equally contributed to this research

#### Ethics

This research is original and contains unpublished material. The corresponding authors confirms that the other author has read and approved the manuscript and no ethical issues involved.

## References

- Bargiel, D., 2017. A new method for crop classification combining time series of radar images and crop phenology information. *Remote Sens. Environ.*, 198: 369-383. DOI: 10.1016/j.rse.2017.06.022
- Baumann, M., M. Ozdogan, T. Kuemmerle, K.J. Wendland and E. Esipova *et al.*, 2012. Using the Landsat record to detect forest-cover changes during and after the collapse of the Soviet Union in the temperate zone of European Russia. *Remote Sens. Environ.*, 124: 174-184. DOI: 10.1016/j.rse.2012.05.001
- Chhetri, R.P., A.B. Elrahman, T. Liu, J. Morton and V.L. Wilhem, 2017. Object-based classification of wetland vegetation using very high-resolution unmanned air system imagery, *Eur. J. Remote Sens.*, 50: 564-576. DOI: 10.1080/22797254.2017.1373602
- Fernández-Manso, A., O. Fernández-Manso and C. Quintano, 2016. SENTINEL-2A red-edge spectral indices suitability for discriminating burn severity. *Int. J. Applied Earth Obs. Geoinf.* 50: 170-175. DOI: 10.1016/j.jag.2016.03.005
- Gao, F., M.C. Anderson, X. Zhang, Z. Yang and J.G. Alfieri *et al.*, 2017. Toward mapping crop progress at field scales through fusion of Landsat and MODIS imagery. *Remote Sens. Environ.*, 188: 9-25. DOI: 10.1016/j.rse.2016.11.004
- Ghassemian, H., 2016. A review of remote sensing image fusion methods. *Inform. Fus.*, 32: 75-89. DOI: 10.1016/j.inffus.2016.03.003
- Hagolle, O., S. Sylvander, M. Huc, M. Claverie and D. Clesse *et al.*, 2015. SPOT-4 (take 5): Simulation of Sentinel-2 time series on 45 large sites. *Remote Sens.*, 7: 12242-12264. DOI: 10.3390/rs70912242
- He, C., B. Gao, Q. Huang, Q. Ma and Y. Dou, 2017. Environmental degradation in the urban areas of China: Evidence from multi-source remote sensing data. *Remote Sens. Environ.*, 193: 65-75. DOI: 10.1016/j.rse.2017.02.027
- Immitzer, M., F. Vuolo and C. Atzberger, 2016. First experience with Sentinel-2 data for crop and tree species classifications in central Europe. *Remote Sens.*, 8: 166-166. DOI: 10.3390/rs8030166
- Kandrika, S. and T. Ravinsankar, 2011. Multi-temporal satellite imagery and data fusion for improved land cover information extraction. *Int. J. Image Data Fus.*, 2: 61-73. DOI: 10.1080/19479832.2010.518166
- Li, X.S., Z. Deng, Z. Chen and Q. Fei, 2011. Analysis and simplification of three-dimensional space vector PWM for three-phase four-leg inverters. *IEEE Trans. Industrial Electron.*, 58: 450-464. DOI: 10.1109/TIE.2010.2046610
- Manaf, S.A., N. Mustapha, M.N. Sulaiman, N.A. Husin and M.R.A. Hamid, 2016. Comparison of classification techniques on fused optical and SAR images for shoreline extraction: A case study at northeast coast of Peninsular Malaysia. *J. Comput. Sci.*, 12: 399-441. DOI: 10.3844/jcssp.2016.399.411
- Navarro, A., J. Rolim, I. Miguel, J. Catalão and J. Silva *et al.*, 2016. Crop monitoring based on spot-5 take-5 and sentinel-1a data for the estimation of crop water requirements. *Remote Sens.*, 8: 525-525. DOI: 10.3390/rs8060525
- Novelli, A., M.A. Aguilar, A. Nemmaoui, F.J. Aguilar and E. Tarantino, 2016. Performance evaluation of object-based greenhouse detection from Sentinel-2 MSI and Landsat OLI data: A case study from Almería (Spain). *Int. J. Applied Earth Obs. Geoinf.*, 52: 403-411. DOI: 10.1016/j.jag.2016.07.011
- Patrick, A.V., K. Spröhnle, C. Geiß, E. Schoepfer and S. Plank *et al.*, 2018. Multi-sensor feature fusion for very high spatial resolution built-up area extraction in temporary settlements. *Remote Sens. Environ.*, 209: 793-807. DOI: 10.1016/j.rse.2018.02.025
- Segl, K., L. Guanter, F. Gascon, T. Kuester and C. Rogass *et al.*, 2015. S2eteS: An end-to end modelling tool for the simulation of sentinel-2 image products. *IEEE Trans. Geosci. Remote Sens.*, 53: 5560-5571. DOI: 10.1109/TGRS.2015.2424992
- Storey, J., D.P. Roy, J. Masek, F. Gascon and J. Dwyer *et al.*, 2016. A note on the temporary misregistration of Landsat-8 Operational Land Imager (OLI) and Sentinel-2 Multi-Spectral Instrument (MSI) imagery. *Remote Sens. Environ.*, 186: 121-122. DOI: 10.1016/j.rse.2016.08.025
- Van der Werff, H. and F. Van der Meer, 2016. Sentinel-2A MSI and Landsat 8 OLI provide data continuity for geological remote sensing. *Remote Sens.*, 8: 883-883. DOI: 10.3390/rs8110883
- Wang, Q., W. Shi, Z. Li and P.M. Atkinson, 2016. Fusion of sentinel-2 images. *Remote Sens. Environ.*, 187: 241-252. DOI: 10.1016/j.rse.2016.10.030
- Wurm, M., H. Taubenbock and M. Schardt, 2011. Object-based image information fusion using multisensor earth observation data over urban areas. *Int. J. Image Data Fus.*, 2: 121-147. DOI: 10.1080/19479832.2010.543934
- Yuhendra, I. Alimuddin, J.T.S. Sumantyo and H. Kuze, 2012. Assessment of pan-sharpening methods applied to image fusion of remotely sensed multi-band data. *Int. J. Applied Earth Observat. Geo- Inform.*, 18: 165-175. DOI: 10.1016/j.jag.2012.01.013
- Yuhendra, J.T.S., 2017. Assessment of multi-temporal image fusion for remote sensing application. *Int. J. Adv. Sci. Eng. Inform. Technol.*, 7: 778-784. DOI: 10.18517/ijaseit.7.3.1676

Zhou, C. and L. Zheng, 2017. Mapping radar glacier zones and dry snow line in the Antarctic peninsula using sentinel-1 images. *Remote Sens.*, 9: 1171-1171. DOI: 10.3390/rs9111171

Zhou, T., Z. Li and J. Pan, 2018. Multi-feature classification of multi-sensor satellite imagery based on dual-polarimetric sentinel-1A, landsat-8 OLI and hyperion images for urban land-cover classification. *Sensors*, 18: 373-373. DOI: 10.3390/s18020373

Zhuang, H., F. Hongdong, K. Deng and G. Yao, 2018. A spatial-temporal adaptive neighborhood-based ratio approach for change detection in SAR images. *Remote Sens.*, 10: 1-19. DOI: 10.3390/rs10081295